Contrasting patterns of thermo-erosion gullies formed in syngenetic ice wedge polygonal terrains on Bylot Island, eastern Canadian Arctic: case studies from three different sedimentary environments

GEOQuébec 2015
Challenges from North to South
Des défis du Nord au Sud

Audrey Veillette, Daniel Fortier & Etienne Godin
Université de Montréal, Montréal, QC, Canada
Centre d'Etudes Nordiques, Université Laval, QC, Canada

ABSTRACT
Ice wedge polygonal terrains, typical of Arctic permafrost geosystems, are vulnerable to thermo-erosional gullying and thermokarst. Gullies located on Bylot Island (NU) have distinct shapes and dynamics on factors such as their age, alluvial activity level, water balance and nature of the sedimentary environment. In this paper we focus on the contrasts differencing gullies observed in aeolian sands, colluvium/alluvium and peaty-loess deposits. Polygons areas, ice wedges size and consequently gully shapes were distinct for each environment: the peaty-loess-zone had medium-sized polygons and generally larger ice wedges, which erosion resulted in well-developed multi-channel gullies. The aeolian sands-zone had smaller polygons and thinner ice wedges, where quasi-linear gullies were formed. The colluvium/alluvium-zone had large polygons with large primary ice wedges. The erosion was concentrated, very active, and essentially restricted to the primary ice wedges. The role of the ice wedges geometry and size in the evolution of the gullies was major, putting thermo-erosion gullies as distinct landforms from gullies found in warmer, non-permafrost zones.

RÉSUMÉ
Le pergélisol parsemé de polygones à coin de glace caractérisant le haut-Arctique est vulnérable au thermokarst et au ravinement. Les ravins (Ile Bylot, NU) ont une dynamique qui dépend de facteurs tels que leur âge, leur stabilité, leur bilan hydrologique et la nature de leur environnement de déposition. Cet article porte sur les contrastes propres aux ravins se trouvant dans des dépôts éoliens sableux, des loess organiques et des colluvions/alluvions. Les ravins dans la zone de loess organiques se sont formés dans des polygones de taille moyenne composés de coins de glace larges, résultant en de grands ravins multi-branches; les polygones et les coins de glace dans la zone de dépôts sableux éoliens étaient petits et les ravins résultants quasi-linéaires; en zone de colluvions, les polygones étaient grands; le nombre d'axes d'érosion était moindre mais chacun particulièrement actifs. Lorsque l'érosion survient, l'organisation et la taille des coins de glace distinguent le processus de ravinement en région de pergélisol par rapport à celui des zones tempérées non pergélisolées.

1 INTRODUCTION

The high Arctic landscape is characterized and influenced by the presence of ice wedges incising permafrost soils, as it is the most distributed form of massive ground ice (Mackay 1972). Ice wedges form over several years as the result of recurrent thermal contraction cracking during cold winter spells and refreezing of snowmelt water in the open cracks in the spring. Repetition of such a sequence over the years leads to the formation of v-shaped massive-ice bodies (Lachenbruch 1962) which represent an important part of the ice content of the upper part of the permafrost (Harry et al. 1988; Jorgenson et al. 2006; Pollard and French 1980; Ulrich et al. 2014). Permafrost susceptibility to thawing and potential for perturbation is intimately linked to its ground ice content ratio and ground composition (Burn and Kokelj 2009; Jorgenson et al. 2006; Kanevskiy et al. 2013; Pollard and French 1980; Rowland et al. 2010). Permafrost soils with ice wedges are therefore susceptible to more instability, even at very low temperatures, due to large amount of ice in the near surface, just below the active layer (Jorgenson et al. 2006).

Thermo-erosion gullies are a permafrost geosystem feature resulting from the thermal and mechanical degradation of ice wedges, induced by water flow into ice wedges and the surrounding permafrost (Fortier et al. 2007; Godin and Fortier 2012d). The melting of the ice through convective heat flow between running water, ice/frozen ground is the main driver of the initial degradation. Underground ice and soil erosion then leads to collapse of sinkholes and tunnels which opens the gully system and exposes the permafrost to radiation and sensible heat. Gully branches undergo retrogressive retreat from the main axis of the gully essentially following the ice wedges system pattern, which often results in a complex thermokarst geomorphology (Fortier et al. 2007; Godin and Fortier 2012a; Godin and Fortier 2012d; Godin et al. 2014; Morgenstern et al. 2013). In a previous study, Godin et al. (2014) demonstrated that rapid terrace incision due to gullying changed runoff circulation from flooding of polygons and lateral flow (pre-gully) to concentrated and channelized flow (near and in the gully). Channelized flow have a quicker transit time through the watershed and doesn't contribute to the hydrological recharge of the active layer of the polygons anymore.

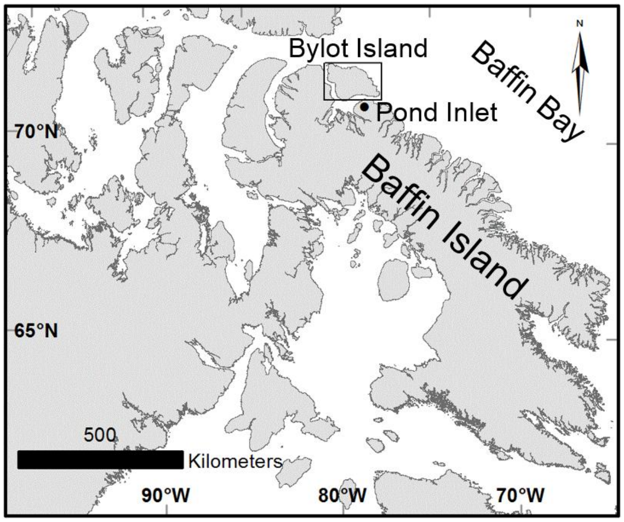

Figure 1 : Bylot Island, Nunavut, Canada.

The study site is located in the Qarlikturvik valley, on the southern plain of Bylot Island, Nunavut (Figure 1). This valley is characterized by extensive well-developed network of ice-wedge polygons that formed on Holocene terraces bordering a proglacial river (Fortier and Allard 2004). Syngenetic ice wedges developed in organic, aeolian and colluvial sediments while epigenetic ice wedges developed in glacial deposits. Active gullies, a few hundred meters up to a few kilometers long, incise and drain the terrace in the pro-glacial river. We compared the geomorphology of gullies and the short-term erosion rates of gully branches in three distinct types of sedimentary environments characterizing the valley floor at the study site: aeolian cover sand, loess and colluvium/alluvium. At all sites, organic matter accumulated synchronously with sedimentary deposition, which implies that the ice wedges are of syngenetic origin. A special attention was paid to the branching patterns of the gullies in order to evaluate the impact of distinct terrain units (sedimentary environments) on gully shape and rates of erosion.

The objectives of the paper are to a) characterize the contrasting three sedimentary environments where thermo-erosion gullies were studied; and b) to define and compare the spatial attributes of the gullies (geometry, permafrost degradation features, extent, active retreat pattern) seen as a network of connected erosion branches linked by ice wedges.

2 STUDY SITES

The Qarlikturvik valley (73°9'N, 79°57'W) is located about 85 km NW of the village of Pond Inlet (Figure 1). The 1981 – 2010 climate normal (Environment Canada 2015) recorded at the Pond Inlet Airport indicated a yearly normal mean air temperature of -14.6˚C, a normal mean precipitation of 189 mm, with 48% falling as rain. The average atmospheric degree days of thawing (DDT) at Pond Inlet was 473 during the latest 1981 – 2010 climate normal period (Environment Canada 2015). The valley at the study site is approximately 65 km^2, over 17 km long, 4 ± 1 km wide and delimited by plateaus approximately 500 m a.s.l. (Godin and Fortier 2012a). The valley is incised by a braided glacio-fluvial river aligned ENE-WSW and supplied by meltwaters from glaciers C-79 and C-93 (Inland Water Branch 1969). On both sides of the river, at the margin of the sandur, the valley floor is characterized by ice-wedge polygons terraces. The terraces at the valley mouth, exposed to the Navy board inlet, are made of aeolian sands deposited over the sparse mesic vegetation. At the base of the valley walls, coarser colluvial sediments form talus and alluvial fan. For the remaining of the valley, most polygons are composed of loess deposited over wet (polygon center) and mesic (polygon ridges) vegetation (Fortier et al. 2006). Thermal-contraction cracking is active (Fortier and Allard 2005) and ice-wedge polygons grow syngenetically with surface sedimentation in the three types of deposits (Figure 2). We conducted a comparative geomorphological study of selected thermo-erosion gullies formed in the valley to evaluate how gully shape and erosion rates varied between different sedimentary environments.

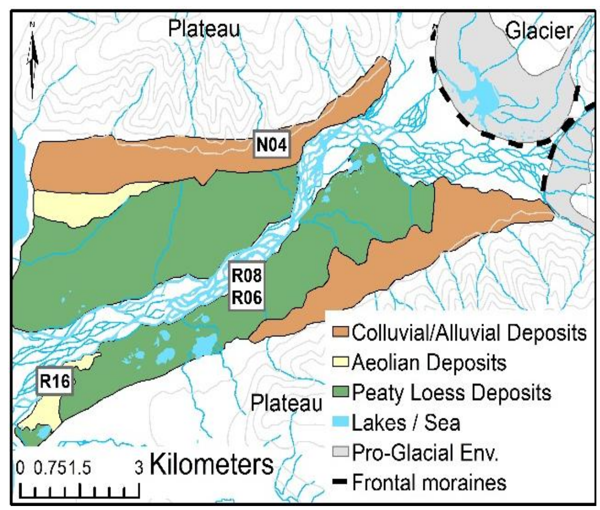

Figure 2. Qarlikturvik valley map of surficial deposits, (modified from Godin and Fortier (2012a)) showing the location of the four studied gullies (R16, R08, R06 and N04)

3 METHODS

The morphological characterization of the gullies was assessed with a particular attention on gullies branches by measuring their frequency, retreat areas, erosion rates, and geomorphological indicators of thermal erosion processes (exposed ice-wedges, retrogressive thaw-slumps, tunnels and collapses). Grain size distribution and the pattern of ice-wedge polygons between sedimentary environments were compared giving hints on ice content, Surface deposits characteristics

			Polygons characteristics					Grain size analysis							
Surface Deposit	Area (km²)	Gully (ies)	Mean size (m²)	Min. size (m²)	Max. size (m²)	Mean width (m)	Mean great axis (m)	Mean ϕ	Sorting (standard deviation)	Graphic skewness	Gravel (%)	Sand (%)	Silt (%)	Clay (%)	Sediment name
Aeolian	2,65	R16	456 n=149	111	2109	20	30	3,8	1,97	-0,56	0	68,1	24,6	7,3	Silty Sand
Peaty Loess	32,90	R08 R06 }	681 n=220	134	2250	26	36	5,0-6,0	1,2-1,8	0,03 - 0,3	0	12,0 - 25,0	70,0 - 83,0	4,0 - 8,0	Silt
Colluvial	14,53	N04	1963 n=35	756	4521	43	64	1,8	1,60	0,05	6	88	5,81	0,19	Gravelly Sand

Table 1. Polygons and surface deposits characteristics of the three sedimentary environments.
*Grain size analysis data for the peaty loess deposits was taken from (Fortier and Allard 2004)
Max. = Maximum; Min. = Minimum

ice wedge distribution and size, vulnerability to thawing and drainage conditions.

3.1 Sediment properties

Grain size analysis of four gullies was performed through sieving and hydrometry of sediments. Gully R16 was formed in coarse aeolian sediment (sand), gully R06 and R08 in fine-grained aeolian sediment (loess and peat), and gully N04 in colluvium/alluvium. Grain size analysis of gullies R06 and R08 sediments was taken from (Fortier and Allard 2004).

3.2 Ice wedge polygons mapping

Low-center polygons contours located near the gullies were mapped by interpretation of high resolution satellite images (GeoEye, early September 2010, 1 pixel = 0.5 m and IKONOS late July 2007, 1 pixel = 1 m). The IKONOS image was used as a reference to characterize N04 since it was masked by clouds on the GeoEye image. Polygons delineation was performed by mapping ice-wedge troughs separating ridges. In the three sedimentary environment all polygons contours located within a rectangular area of 0.3 km² were mapped. The rectangular shape was selected arbitrarily to ease comparisons and the selected surface was the maximum area fitting the smallest sedimentary environment (aeolian sands) without encroaching other deposits or water bodies. This area represented 11.45% of the area covered by active aeolian deposits, 2.09% of the area covered by colluvial/alluvial deposits and 0.92% of the area covered by peaty loess deposits. Polygons area, width and long axis were measured using the “Calculate Geometry tool” and “Minimum Bounding Geometry” under the “Convex Hull” geometry type, in ArcMap 10.2. Width and long axis correspond, respectively, to the shortest and longest line between two polygonal troughs.

3.3 Gully Mapping

The morphology of the four gullies was mapped in the field using a differential GPS (GNSS Trimble model R8) with a centimeter precision. Field mapping consisted in following the edges of each gully to quantify the area directly affected by thermo-erosion. Most stabilized areas previously affected by thermo-erosion and baydzherakhii were mapped only if recent signs of mechanical and/or thermal erosion were visible (e.g. running water, no colonization by vegetation, steep slopes). Comparing mapped areas from previous years (2010-2013) provided the increased area affected by gullying. Considering stabilization processes and subjectivity of the GNSS operator, mapping data were validated with linear retreat measurements for a better precision of retreat rates. Each year (2010 to 2013) erosions stakes were placed at a distance of 5 meters from the gully branches edges. With a measuring tape, we measured the distance of those stakes to the border of the gully branch the following year. This method gave us data on the dynamics of the branches rather than the dynamic of the gully as a whole. Linear retreat measurements have been measured since 2010, allowing for an estimation of the mean short term linear retreat rate of the branches for each gully. Absent stakes revealed retreat of more than 5 meters in some highly active erosion zones. Where that happened, GNSS survey was particularly useful to estimate the retreat. Comparing this mean linear retreat rate to each individual branch of a gully permitted the localization of critical eroding areas.

4 RESULTS AND DISCUSSION

Thermo-erosion gullies, as gullies formed in non-permafrost environments, have distinct morphologies in function of the host material properties (Rowntree 1991) related to their specific sedimentary environment.

4.1 Sedimentary environments

Figure 3 shows the three distinct sedimentary environments comprising the thermo-erosion gullies studied in the Qarlikturvik valley (Figure 3). Ice wedges are ubiquitous throughout these three environment and developed under different frozen ground conditions. The four thermo-erosion gullies studied depend upon ice wedges presence, which geometry and abundance is function of surficial material.

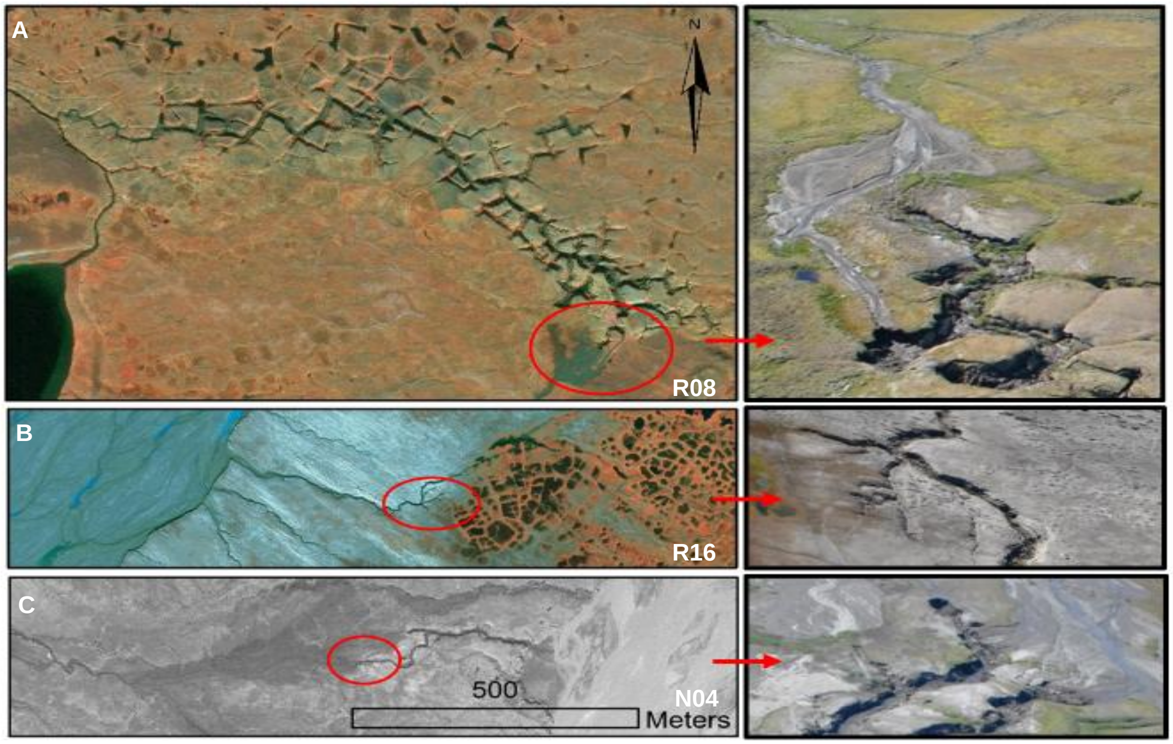

Figure 3. Satellite imagery of gullies in their sedimentary environment and associated aerial photography of gullies head. A) Gully R08 incising the peaty loess deposit; B) Gully R16 incising the sandy aeolian deposit; and C) Gully N04 incising the colluvial/alluvial deposit. Gullies R08 and R16 are represented on the GeoEye imagery (2010) and gully N04 is represented on the IKONOS imagery (2007).

4.1.1 Aeolian cover sands and silts sedimentary environment

The active, aeolian and sand environment extends over 2.65 km² from the coast of Navy Board Inlet up to a low-centered polygons area where small ponds are ubiquitous. The area is very poorly vegetated with patches of bare ground. The environment is dominated by sands (~ 68%) and silts are an important part of the grain size distribution (Table 1). This aeolian sedimentary environment results from strong summer westerly prevailing winds blowing over the glacio-fluvial outwash. As the winds enter the valley, they decelerate and deposit their coarser sediment load (Fortier et al. 2006). Ice-wedge polygons are observable in the field and via satellite imagery. However, the polygonal pattern is poorly expressed since cracks, ridges and troughs are continuously filled or covered with sands. Such environment hosts little to no vegetation, thus enabling strong sand remobilization throughout the non-cohesive substratum (Pissart et al. 1977). The mean polygon surface-area was the smallest of all three environments with 455 m² estimated from 146 polygons. The polygons show a variation in surfaces range following a standard deviation of 281 m², a maximum of 2109 m² and a minimum of 111 m². The polygons shapes are elongated; the mean ratio between the long axis and the width is 1.48. Drier and coarser environments tends to host larger polygons but interestingly this active aeolian sedimentary environment hosts the smallest mean surface area of polygons. Brown (1967), demonstrated that very low ice content reduces considerably soil tensile strength, so that thermal cracks, and therefore ice wedges, can be spaced more closely. Alternatively, the small polygon size might be the heritage of past conditions when the polygonal network developed (Plug and Werner 2002). Indeed, the thermal stress present during the initial formation of the polygonal network are the main determinant of its current configuration although colder climate conditions (e.g. Little Ice Age) may be conducive to formation of additional ice wedges. Considering that aeolian sands have smaller coefficient of thermal contraction than ice-rich peaty loess, then under the current conditions, ice wedge cracking in aeolian sands likely occurs less often than in the peaty loess (Fortier and Allard 2004) The smaller width of the ice wedges in aeolian sands is reflected by the gully width, which is strongly function of the size of ice wedges eroded (Fortier et al. 2007) (Figure 3).

4.1.2 Peaty Loess Sedimentary Environment

This environment is the most widespread throughout the valley representing about ±33 km². Loess are deposited in well-vegetated polygons which results in an ice-rich mixture of poorly-decomposed peat and loess (Fortier et al. 2006). The polygonal terraces border the glacio-fluvial river and are limited North and South by slope deposits (Figure 2). Previous grain size analysis conducted in the surrounding area revealed a strong silty fraction (70-83%) with few sand and very few clay (Table 1) (Fortier and Allard 2004). Fortier et al. (2006) suggested that the loess deposition is due to deceleration of summer westerly prevailing winds channeled in the valley. Consequently, the gradation from fine sand on the coast towards silt (loess) further in the valley follows a well-defined spatial pattern. The ice-wedge polygons are clearly defined by differences in vegetation patterns and contrasted troughs-ridge pattern. The mean polygon size in the rectangular sampling zone located in low-center polygons was estimated to be ± 680 m² with the smallest having an area of 133 m², the widest 2250 m² and a standard deviation of 350 m² (Table 1). The shape of the polygons was elongated similarly to the aeolian environment, with a mean ratio of 1.42 between long axis and width. Ice-rich peaty silt and silty peat deposit have high coefficient of thermal contraction and expansion (Fortier and Allard 2005; Gray and Seppala 1991; Kerfoot 1972). Frost cracking of ice wedges is common and is illustrated by the well-developed ridges and troughs forming a dense network of polygons (220 in 0.3 km²). Ice wedges are larger than in aeolian sands as shown by the size of gully branches. Polygonal troughs forms preferential run-off flowpaths (Levy et al. 2008; Liljedahl et al. 2012; Woo and Guan 2006), which are the drivers of thermo-erosion of ice-wedges and subsequent permafrost degradation features.

4.1.3 Gravelly Sands Colluvium/Alluvium Sedimentary Environment

At the base of the plateaus there are vast colluvium/alluvium complex of gravelly sands deposits generated by slope and intermittent alluvial processes. The area covers ±14 km² and is partly vegetated with patches of bare soil close to the disturbed/gullied areas. Grain size analysis revealed a dominance of gravelly sand (94%) spread over alluvial fans formed down long gullies incised in beds of sandstone and shales (Table1). The mean polygon area was larger than in the two aeolian-derived sedimentary environments with 1963 m² ± 931 m² (n=35 polygons), showing that coarser sediments host larger polygons (Dostovalov and Popov 1966; Harry et al. 1988). The smallest polygon was 756 m² and the widest 4521 m², although smaller polygons were observed outside of the rectangular sampling area. The mean ratio between the long axis and the width of polygons was 1.48. The polygonal terrain is characterized by longitudinal ice wedges following the slope of alluvial fan channels. These wedges can be large because they are the preferential zones of thermal cracking; the cracks often propagating towards all the wedge length (Fortier and Allard 2005). This is illustrated by the width of the gully and observations of exposed ice wedges at the gully head.

4.2 Gullies Morphology and Retreat

As thermo-erosion gullies are impacting the periglacial landscape by disturbing hydrologic and topographic components (Godin et al. 2014; Morgenstern et al. 2013), it is crucial to better understand the range of morphologic traits of these landforms. Results from different sedimentary environments showed that ice wedge polygons had variable morphology. Thermo-erosion gullies and their branches essentially followed these ice wedges polygonal pattern (Godin and Fortier 2012d).

Morphologic characteristics

Gully name	Area (m²)	Gully floor slope (°)	Erosion axes	*Gully morphology and erosion activity
R16	4095	0.008	13	
R08	24800	0.013	94	
R06	14908	0.017	47	
N04	7366	0.012	10	

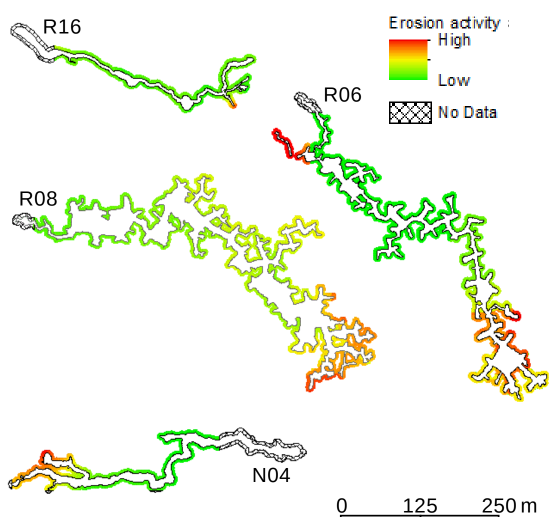

Table 2 Morphologic characteristics of 4 gullies and their erosion activity. The outlet of gullies outlet is located where the gully name appears.

4.2.1 Aeolian Cover Sands and Silts Sedimentary Environment (Gully R16)

Gully R16 is one of eight other gullies incising the poorly vegetated sands of the southern active aeolian sedimentary environment. The gully shape was mostly linear with 13 erosion branches incised in surficial deposits in an NW-ESE direction and limited downstream (NW) by the glacio-fluvial river and upstream (SE) by a vegetated low-centered polygons area. The main slope of the gully floor was 0.01°. Apart from the main channel, only 4 main erosion branches were well developed at the gully head, where water flowing from low centered polygons entered the gully system (Figure 3). These branches showed the highest erosion activity of the gully (Tab. 2) and converged into the main channel flowing into the river (Figure 3). The other erosion branches were mostly the result of mechanical erosion and were barely observable on satellite imagery making them distinct than thermo-erosion gully branches which are larger (Figure 3). R16 was the smallest mapped gully with an area of 4095 m² in 2013. During our fieldwork operations, from 2010 to 2013, no signs of exposed ice wedge, tunnel or retrogressive slumping were observed. The linear morphology of R16 is attributed to a limited and localized source of water entering the system, restraining thermo-erosion expansion. The absence of thermokarst processes elsewhere along the gully suggests the limited impact of radiative and atmospheric heat transfer processes in the sands, potentially reflecting a poor ice content, hence the low thawing susceptibility of the sediment enclosing the ice wedges.

Figure 4. Roof collapse at the outlet of gully R06 in the summer of 2013, showing exposed ice wedges and thawed active slumps material.

Figure 5. Thermo-erosion tunnel incised in sediments at gully site N04 in the summer of 2013.

4.2.2 Peaty Loess Sedimentary Environment (Gullies R06 and R08)

Both gullies R08 and R06 located in the peaty loess sedimentary environment showed numerous branches and erosion axes (94 and 47, respectively). Over the whole peaty loess deposit, a number of 13 thermo-erosion gullies were observed (Godin et al. 2014). These two gullies were amongst the largest in the valley (24800 m² for R08 and 14908 m² for R06 in 2013, for channels and branches only, excluding some baydzherakhii and ground settlements zones). Both R08 and R06 has developed in an overall NE-SO direction, reflecting run-off patterns. The main slope of the gully floor is 0.01° for R08 and 0.02° for R06. The upstream sections of R08 and R06 are actively eroding (Table 2) where water running down the southern slope enters the system preferentially (Figure 3). Water inlets were also observed on the eastern side of gully R08, as reflected in the erosion activity pattern (Table 2). Erosion activity at R06 (Table 2) highlights the non-linear relation between water inlets and erosion. Indeed, gully heads are active, but so is the outlet of R06, where a major tunnel collapse appeared in the summer of 2013 (Figure 4). The elevated number of erosion branches and sizes of the gullies could be attributed to the generally higher ice-content of frozen silt and the large size of the ice wedges. This high ice content increased the susceptibility to thawing once thermo-erosion and roof collapse exposed new soil to solar radiation and sensible heat. In fact, tens of retrogressive thaw slumps, a few tunnels and exposed ice wedges were observed for each gully during our 2010-2013 surveys. The density of ice wedges and associated troughs created preferential flow paths for surface run-off, therefore enhancing thermo-erosion processes.

4.2.3 Gravelly Sands Colluvium/Alluvium Sedimentary Environment

Gully N04 is located at the foot of the northern slope of the valley and extends to the glacio-fluvial river (Figure 3). Nine thermo-erosion gullies were observed in this colluvial/alluvial environment. The gully N04 has a very linear system developed in coarse gravelly sands over an area of 7366 m² (2013) oriented West to East. The slope of the gully floor is 0.01°. Ten erosion axes were observed over the whole gully. Only four branches were eroding away from the main gully axis, but the erosion was highly active. In 2013, three thermo-erosion tunnels were observed (Figure 5). Interestingly, some of these tunnels were incised into sediments enclosing ice wedges rather than in the ice wedges themselves which is usually the case. The head of gully N04 was a very active eroding zone. The retreat increased abruptly from 2010 to 2013, where the main two branches located at the gully head retreated by 116 m over two years (2011-2013). This is tentatively explained by the coarse nature of the sediments which favors quick-flow through the active layer and easier access to ice wedges (Jorgenson et al. 2010).

5 CONCLUSION

The comparative study of thermo-erosion gullies showed that sedimentary environments have an incidence on geomorphology and erosion patterns of this landform. Heterogeneity was observed through erosion features, erosion branches, size, and erosion activity patterns. A variety of morphology has also been reported for gullies in non-permafrost areas although gully shape depends on numerous other factors as well (Billi and Dramis 2003; de Oliveira 1989; Rowntree 1991; Wishart and Warburton 2001). The slope of gully floor (0.01°-0.02°) was gentle which indicates that thermo-erosion gullies erosion is mainly driven by the density of ice wedges patterns and water inflow, rather than mechanical erosion due to steeper slopes. In non-permafrost terrains, slopes are strongly related to gully development since it favours rills initiation and further gully formation (Valentin et al. 2005). However, in ice wedge polygonal terrains, rills develop on flat terrain and are ubiquitous due to troughs formed between polygon ridges.

The erosion activity patterns of the gullies were variable among the four studied features. The gully in aeolian sand was mostly linear with localized erosional activity along small ice wedges. The gullies in peaty loess were very well-developed, had numerous branches sustaining high erosion rates along large ice wedges. The gully in colluvium/alluvium was mostly linear, with few erosion branches sustaining very high erosion rates along large ice wedges. All gullies presented high relative activity where water entered the system. Processes like reactivation of gully branch at the outlet indicates that mechanisms of stabilization can be momentarily disrupted and erosion re-activated. It was observed that thermokarst disturbances post thermo-erosion processes was larger for dense polygonal patterns with large ice wedges.

The conclusions from these case-study provide hypothesis to be tested at the landscape scale.

ACKNOWLEDGEMENTS

We are grateful to S. Coulombe and G. Létourneau for their help in the field. We also thank the team of Prof. G. Gauthier (U. Laval) and the staff of the Sirmilik National Park for logistical support and access to Bylot Island. This project was funded by ArcticNet, the Natural Sciences and Engineering Research Council of Canada (NSERC), the Fonds de recherche du Québec – Nature et technologies (FRQNT), the Polar Continental Shelf Program (PCSP) of Natural Resources Canada, the Northern Scientific Training Program (NSTP) of the Canadian Polar Commission, the NSERC Discovery Frontiers grant 'Arctic Development and Adaptation to Permafrost in Transition' (ADAPT).

REFERENCES

Billi, P., and Dramis, F. 2003. Geomorphological investigation on gully erosion in the Rift Valley and the northern highlands of Ethiopia. CATENA 50(2–4): 353-368.

Brown, J. 1967. Tundra Soils Formed over Ice Wedges, Northern Alaska. Soil Science Society of America Journal 31(5): 686-691.

Burn, C.R., and Kokelj, S.V. 2009. The environment and permafrost of the Mackenzie Delta area. Permafrost and Periglacial Processes 20(2): 83-105.

de Oliveira, M.A.T. 1989. Erosion disconformities and gully morphology: A threedimensional approach. CATENA 16(4–5): 413-423.

Dostovalov, B.N., and Popov, A.I. 1966. Polygonal systems of ice-wedges and conditions of their development. *In* First International Conference on Permafrost. National Academy of Sciences-National Research Council, Lafayette, Indiana, United States pp. 102-105.

Environment Canada. 2015. Canadian Climate Normals, 1981 - 2010. Pond Inlet [Online Database]. Available from http://climate.weather.gc.ca/climate_normals/ [accessed March 15 2015].

Fortier, D., and Allard, M. 2004. Late Holocene syngenetic ice-wedge polygons development, Bylot Island, Canadian Arctic Archipelago. Canadian Journal of Earth Sciences 41(8): 997-1012.

Fortier, D., and Allard, M. 2005. Frost-cracking conditions, Bylot Island, Eastern Canadian Arctic Archipelago. Permafrost and Periglacial Processes 16(2): 145-161..

Fortier, D., Allard, M., and Pivot, F. 2006. A late-Holocene record of loess deposition in ice-wedge polygons reflecting wind activity and ground moisture conditions, Bylot Island, eastern Canadian Arctic. Holocene 16(5): 635-646.

Fortier, D., Allard, M., and Shur, Y. 2007. Observation of rapid drainage system development by thermal erosion of ice wedges on Bylot island, Canadian Arctic Archipelago. Permafrost and Periglacial Processes 18(3): 229-243.

Godin, E., and Fortier, D. 2012a. Fine-Scale Spatio-Temporal Monitoring of Multiple Thermo-Erosion Gully Development on Bylot Island, Eastern Canadian Archipelago. *In* Proceedings of the Tenth International Conference on Permafrost. *Edited by* K.M. Hinkel. The Northern Publisher Salekhard, Salekhard, Yamal-Nenets Autonomous District, Russia. pp. 125-130.

Godin, E., and Fortier, D. 2012d. Geomorphology of a thermo-erosion gully, Bylot Island, Nunavut, Canada. Canadian Journal of Earth Sciences 49(8): 979-986.

Godin, E., Fortier, D., and Coulombe, S. 2014. Effects of thermo-erosion gullying on hydrologic flow networks, discharge and soil loss. Environmental Research Letters 9(10): 105010.

Gray, J.T., and Seppala, M. 1991. Deeply dissected tundra polygons on a glacio-fluvial outwash plain, Northern Ungava Peninsula, Quebec. Geographie Physique Et Quaternaire 45(1): 111-117.

Harry, D.G., French, H.M., and Pollard, W.H. 1988. Massive ground ice and ice-cored terrain near Sabine Point, Yukon Coastal Plain. Canadian Journal of Earth Sciences 25(11): 1846-1856.

Inland Water Branch. 1969. Bylot Island Glacier Inventory: Area 46201. *In* Glacier Atlas of Canada. *Edited by* Inland Water Branch. Department of Energy, Mines and Resources, Ottawa. p. 76.

Jorgenson, M.T., Romanovsky, V., Harden, J., Shur, Y., O'Donnell, J., Schuur, E.A.G., Kanevskiy, M., and Marchenko, S. 2010. Resilience and vulnerability of permafrost to climate change. Canadian Journal of Forest Research 40(7): 1219-1236.

Jorgenson, M.T., Shur, Y.L., and Pullman, E.R. 2006. Abrupt increase in permafrost degradation in Arctic Alaska. Geophysical Research Letters 33(2): F02S17.

Kanevskiy, M., Shur, Y., Jorgenson, M.T., Ping, C.L., Michaelson, G.J., Fortier, D., Stephani, E., Dillon, M., and Tumskoy, V. 2013. Ground ice in the upper permafrost of the Beaufort Sea coast of Alaska. Cold Regions Science and Technology 85(0): 56-70.

Kerfoot, D.E. 1972. Thermal contraction cracks in an arctic tundra environment. Arctic: 142-150.

Lachenbruch, A. 1962. Mechanics of Thermal Contraction Cracks and Ice-wedge Polygons in Permafrost. Geological Society of America Special Papers. 70.

Levy, J.S., Head, J.W., and Marchant, D.R. 2008. The role of thermal contraction crack polygons in cold-desert fluvial systems. Antarct. Sci. 20(6): 565-579.

Liljedahl, A., Hinzman, L., and Schulla, J. 2012. Ice-wedge polygon type controls low-gradient watershed-scale hydrology. *In* Proceedings of the Tenth International Conference on Permafrost. pp. 231-236.

Mackay, J.R. 1972. Offshore Permafrost and Ground Ice, Southern Beaufort Sea, Canada. Canadian Journal of Earth Sciences 9(11): 1550-1561.

Morgenstern, A., Ulrich, M., Günther, F., Roessler, S., Fedorova, I.V., Rudaya, N.A., Wetterich, S., Boike, J., and Schirrmeister, L. 2013. Evolution of thermokarst in East Siberian ice-rich permafrost: A case study. Geomorphology 201(0): 363-379.

Pissart, A., Vincent, J.S., and Edlund, S.A. 1977. Dépôts et phénomènes éoliens sur l'île de Banks, Territoires du Nord-Ouest, Canada. Canadian Journal of Earth Sciences 14(11): 2462-2480.

Plug, L.J., and Werner, B.T. 2002. Nonlinear dynamics of ice-wedge networks and resulting sensitivity to severe cooling events. Nature 417(6892): 929-933.

Pollard, W.H., and French, H.M. 1980. A first approximation of the volume of ground ice, Richards Island, Pleistocene Mackenzie Delta, Northwest Territories, Canada. Canadian Geotechnical Journal 17(4): 509-516.

Rowland, J.C., Jones, C.E., Altmann, G., Bryan, R., Crosby, B.T., Hinzman, L.D., Kane, D.L., Lawrence, D.M., Mancino, A., Marsh, P., McNamara, J.P., Romanvosky, V.E., Toniolo, H., Travis, B.J., Trochim, E., Wilson, C.J., and Geernaert, G.L. 2010. Arctic Landscapes in Transition: Responses to Thawing Permafrost. Eos Trans. AGU 91(26).

Rowntree, K.M. 1991. Morphological characteristics of gully networks and their relationship to host materials, Baringo District, Kenya. GeoJournal 23(1): 19-27.

Ulrich, M., Grosse, G., Strauss, J., and Schirrmeister, L. 2014. Quantifying Wedge-Ice Volumes in Yedoma and Thermokarst Basin Deposits. Permafrost and Periglacial Processes 25(3): 151-161.

Valentin, C., Poesen, J., and Li, Y. 2005. Gully erosion: Impacts, factors and control. CATENA 63(2-3): 132-153.

Wishart, D., and Warburton, J. 2001. An assessment of blanket mire degradation and Peatland Gully development in the Cheviot Hills, Northumberland. Scottish Geographical Journal 117(3): 185-206

Woo, M.K., and Guan, X.J. 2006. Hydrological connectivity and seasonal storage change of tundra ponds in a polar oasis environment, Canadian High Arctic. Permafrost and Periglacial Processes 17(4): 309-323.